MATERIALS SCIENCE

# Enhanced activity and self-regeneration in dynameric cross-linked enzyme nanoaggregates

**Rui Wang[1,2], Shang Wang[2]†, Jinghua Chen[1], Yan Xu[2], Xiaowei Yu[2]*, Mihail Barboiu[3]*, Yan Zhang[1]***



**Directed evolution, enzyme design, and effective immobilization have been used to improve the catalytic activity. Dynamic polymers offer a promising platform to improve enzyme activity in aqueous solutions. Here, amphiphilic dynamers and lipase self-assemble into nanoparticles of 150- to 600-nanometer diameter, showing remarkable threefold enhancement in catalytic activity. In addition, they also demonstrated the ability to promote the reversible refolding of the partially or completely denatured lipase. The catalytic efficiency is completed with its more convenient handling of dynameric nanoparticles facilitating the efficient recovery and reuse of the enzyme with cost-effective uses. Molecular simulation studies revealed an in-depth understanding of how the dynamer action mechanism affects the conformational changes of lipase. The dynamer served as an effective hydrophobic support, facilitating the lid opening and substrate access to the catalytic triad, resulting in a substantial activation with an improved stability and recyclability of the lipase.**

## INTRODUCTION

Enzymes play a crucial role in biotechnology owing to their high catalytic efficiency and environmental friendliness (*1*–*4*). Among the various types of enzymes, lipase (EC 3.1.1.3) is notable for its high activity and stability. It catalyzes long-chain triglyceride hydrolysis, as well as ester synthesis and exchange reactions, making it one of the most widely used enzymes in the food/oil, pharmaceutical, paper/leather, and cosmetic industries (*5*–*9*). Effective strategies, including directed evolution (*10*–*12*), rational protein design (*13*–*16*), enzyme immobilization and cross-linking (*17*–*20*), and chemical modification (*21*–*23*) have been used to improve the performance of lipases and reduce costs. Although they have been proven very useful and successful, they always require time-consuming molecular-level mutagenesis, massive amounts of screening work, in-depth structural analysis, and complex modification processes.

In our previous studies, we reported a breakthrough simple methodology using dynamic polymers (dynamers), which can be directly added into aqueous reactions, markedly improving the activities of the enzyme (*24*–*26*). We postulated that the noncovalent or reversible covalent interactions with the adaptive dynamers induced the cross-linked enzyme aggregates in the reaction solutions, resulting in higher enzyme loading and activity, biomimetic stabilization, and low carrier loadings. The adaptive dynameric cross-linked enzyme aggregates (dCLEAs) have been illustrated for both carbonic anhydrase and lipase, showing great activation effects in solution, which suggests their suitability for wider applications (*18*, *27*, *28*).

The key challenge in the construction of such dCLEA systems is ensuring gentle interactions between the encapsulating dynameric cross-linkers and the enzyme. This prevents deactivation/denaturation which frequently observed with the enzyme encapsulation in more glassy matrixes. In any of our previous studies, the dynameric cross-linking occurred in aqueous solutions with important enhancements of the enzymatic activity. Fundamentally, the catalytic efficiency of the enzyme must be completed with its more convenient handling within solid nanoparticles rather than a liquid formulation providing a facile separation/decontamination from the product. We postulate that one of creative strategies for addressing these challenges and to achieve improved performances in terms of both catalytic activity and stability, facilitating the efficient recovery and reuse of the enzyme with cost-effective uses, is to generate the dCLEAs within protective nanoparticles for further applications.

Here, we used a series of amphiphilic dynamers, which contain both hydrophilic and hydrophobic components that cross-link lipase, resulting in the production of scalable dynamer-lipase nanoparticles that remarkably outperform the enzyme activity in solution. In addition, we analyzed the aggregation and the conformational changes of lipase through dynameric particle size detection and fluorescence quenching in solution. Moreover, we have also explored the impacts of dynameric enzyme nanoparticles on thermally and chemically denatured lipases during their refolding process. Furthermore, the molecular dynamic (MD) simulations were used to investigate the potential influences of dynamer addition on lipase catalysis, particularly focusing on the conformational changes in the pocket region for interfacial activation. These diverse investigation angles may lead to deeper and unexplored functions of dynameric cross-linking phenomena for lipase activation/reactivation.

## RESULTS

### Dynamer synthesis and characterization

Rhizopus chinensis lipase proRCL from *Rhizopus chinensis* CCTCC M201021 was chosen as the target enzyme (*29*). The gene (GeneBank accession no. EF405962) of proRCL was cloned from *Rhizopus chinensis* CCTCC M201021 and expressed at high levels in *Pichia Pastrois1*. Despite enhancements in expression levels and thermostability achieved through genetic engineering, the performance of proRCL in the papermaking industry remains preliminary. Thus, in addition to genetic method, we propose using a crowding/cross-linking strategy to enhance the lipase performances via its adaptive

[1]Key Laboratory of Carbohydrate Chemistry and Biotechnology, Ministry of Education, School of Life Sciences and Health Engineering, Jiangnan University, Wuxi, 214122, P.R. China. [2]Key Laboratory of Industrial Biotechnology of Ministry of Education, School of Biotechnology, Jiangnan University, Wuxi, Jiangsu, 214122, P.R. China. [3]Adaptive Supramolecular Nanosystems Group, Institut Européen des Membranes, University of Montpellier, CNRS UMR 5365, ENSCM, Place Eugène Bataillon, CC 047, F-34095 Montpellier, France.
*Corresponding author. Email: zhangyanyz@jiangnan.edu.cn (Y.Z.); mihail-dumitru.barboiu@umontpellier.fr (M.B.); yuxw@jiangnan.edu.cn (X.Y.)
†Present address: Dalian Institute of Chemical Physics Chinese Academy of Sciences School of Biological Engineering, Dalian Polytechnic University, XGCJ + 99C, Aizhi Rd, Gan Jing Zi Qu, Da Lian Shi, Liao Ning Sheng, 116039, P.R. China.

gentle entrapment using reversible interactions in self-protecting dynameric lipase nanoparticles. Substantial activity enhancement as well as enzyme lifetime improvement may lead to important production increase and reduced manufacturing costs in industry. Therefore, imine-linked dynamers **P1** and **P2** have been synthetized by using benzene-1,3,5-tricarbaldehyde (**1**) cores and hydrophilic PEG-bis-(3-aminopropyl)-terminated (**2**, PEG, number-average molecular weight ~ 1500) and two different hydrophobic 1,6-hexanediamine (**3**) and 1,12-dodecanediamine (**4**), respectively (Fig. 1A). The molar ratio between **1**:**2**:**3**/**4** was set as 1:0.75:0.75, achieving steady equilibrium after 24 hours at 60°C. Moreover, a hydrophilic dynamer (**P0**) was generated as a reference with a molar ratio between **1**:**2** of 1:1.5. The hydrophobic functional groups within the amphiphilic dynamers were used to facilitate the enzyme lid opening and the access to the active site (*24*, *25*). The linker was used to confer good solubility in water and compatibility with the hydrophilic regions of the enzyme. Conjugation with high molecular hydrophilic poly(ethyleneglycol) (PEG) is often used to enhance protein stability in water, but it has a detrimental effect on their activity. We postulated that connecting low molecular PEG frameworks can accommodate both stability and activity.

The structural analysis of the dynamers in $D_2O$ by nuclear magnetic resonance spectrometry (fig. S1) showed the disappearance of the peak of the aldehyde groups of **1**, confirming the successful generation of dynamers through imine formation reaction. Imine bond exchanges can occur with the amino groups on the surface of lipases, enforcing the noncovalent hydrophobic or hydrophilic interactions between dynameric segments and enzyme surfaces (Fig. 1B). The hydrolytic stability of imine bonds in dynameric systems is high at slightly acidic and neutral pH in aqueous solution. We have previously demonstrated that PEG or alkyl vicinal chains may limit the diffusion of water to the reaction side, providing a protective effect (*24*–*26*). Gel permeation chromatography (GPC) revealed that the apparent molecular weights of the dynamers **P0** to **P2** were 8288, 8457, and 5090 g/mol, respectively, with polydispersity indices of 1.876, 1.527, and 1.223, indicating the presence of a single species in solution (table S1).

## Dynameric cross-linked lipase aggregates

To investigate the morphology of lipase-dynamer complex in solution, the mixture was subjected to dynamic light scattering (DLS) particle size analysis. Initially, a 50 μM lipase solution in phosphate-buffered saline (PBS; 50 mM) was analyzed as the reference, resulting in a particle size of 2000 to 3000 nm, reminiescent with the protein cluster formation via lipase aggregation in solution. Then, increasing amounts of each dynamer were added to the lipase solution. At very low concentration of dynamers, such as 0.5 μM, substantially smaller particle sizes (800 to 1000 nm) were observed, suggesting partial encapsulation of lipase by the interacting dynamers, which affected the

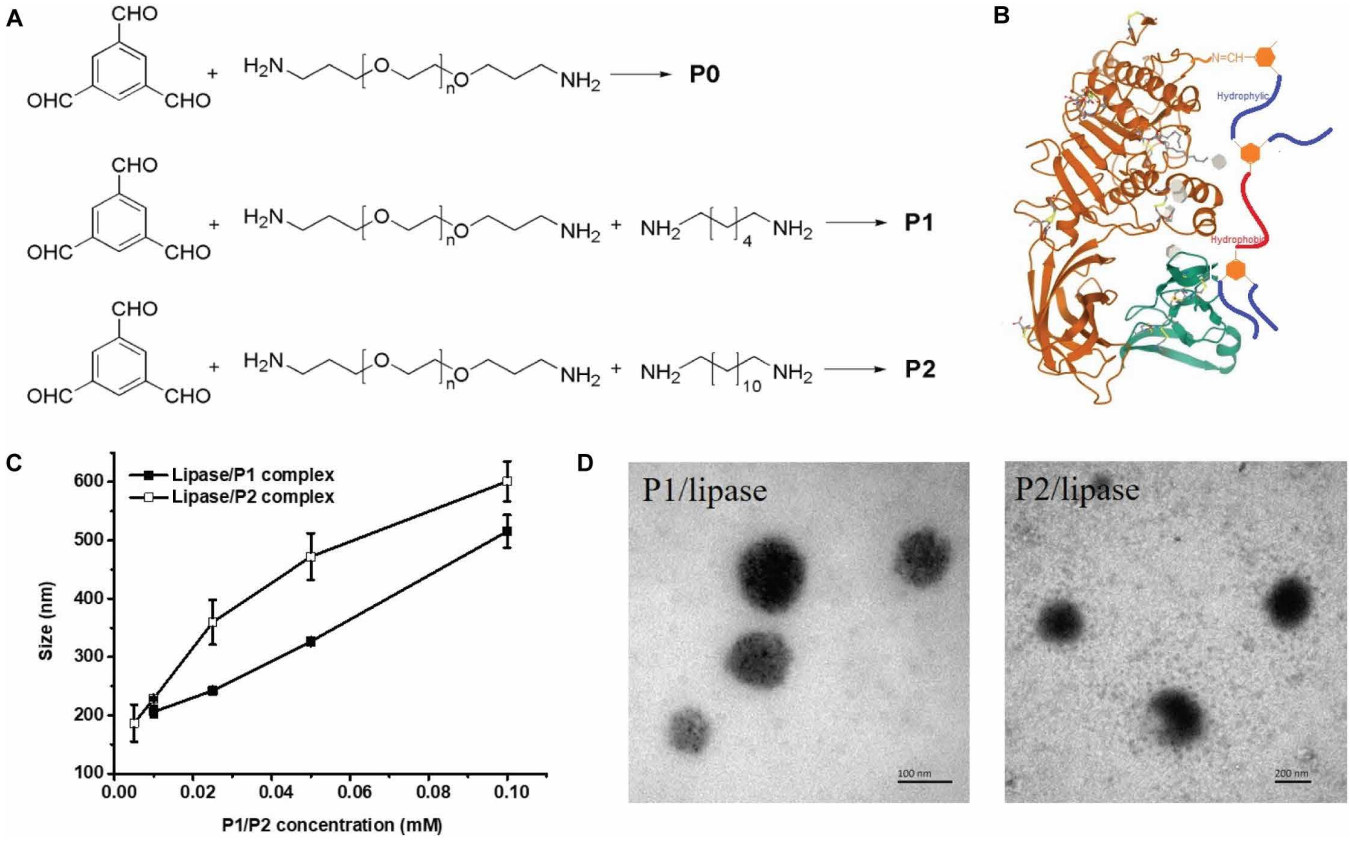


**Fig. 1. Synthesis and characterization of the dynamers.** (**A**) Synthesis of hydrophilic reference **P0** and hybrid amphiphilic **P1** and **P2** dynamers via amino-carbonyl/imine reversible chemistry. (**B**) Lipase-dynamer interactions: imine bonds formation with amino groups on the surface of lipases and hydrophobic and hydrophilic interactions. (**C**) DLS experiments showing the size of the nanoparticles formed by lipase and increasing amounts (0.005 to 0.1 mM) of **P1** or **P2**. (**D**) TEM images of **P1** (0.01 mM)/lipase and **P2** (0.01 mM)/lipase nanoparticles in water.

enzyme self-aggregation. When the concentration of dynameric solution reached a critical value (i.e., 0.01 mM for **P1** and 0.0025 mM for **P2**), the lipase was completely encapsulated and dispersed, forming smaller nanoparticles of 100 to 200 nm. The nanoparticle size progresively increased to a maximum value of 500 to 600 nm when the dynamer concentration raised up to 0.1 mM of **P1** or 0.05 mM of **P2** (Fig. 1C and fig. S2A). When the amount of dynamers exceeded a certain threshold, pure dynameric nanoparticles of 150 to 250 nm (bars in fig. S2A) became predominant in solution, similar to reference pure dynameric solutions presenting the same values across the entire concentration range (lines in fig. S2A).

The reference homodynamer **P0** did not form stable particles for whole range of tested concentrations, confirming that heterogeneous nucleation and the formation of dynamer lipase nanoparticles were only promoted by amphiliphic dynamers. The minimum concentration required to form stable **P1**-lipase nanoparticles was two times higher than that of **P2**, indicating stronger binding of more hydrophobic **P2** to lipase.

Transmission electron microscopy (TEM) confirmed that, compared to the reference dynamers **P1** or **P2** (0.01 mM), for which spherical nanosized particles around 75- to 150-nm diameter were observed in water (fig. S2, B and C), the **P1**-lipase and **P2**-lipase complexes formed spherical nanoparticles with larger diameters of around 100 to 200 nm (Fig. 1D), indicating the encapsulation of lipase into **P1** or **P2**.

## Lipase activation with the dynamers

The hydrolytic reaction of *p*-nitrophenol palmitate (*p*NPP), which produces *p*-nitrophenol (*p*NP), was chosen to evaluate the influences of **P0**, **P1**, or **P2** dynamers on the catalytic activity of lipase (*30*, *31*). In the following experiments, increasing amounts of dynamers were added into the ultraviolet (UV) cuvette containing 100-U lipase and the substrate *p*NPP. The UV absorbance of *p*NP at 410 nm was recorded at the time intervals of 2, 5, and 10 min, to monitor the reaction rates at different stages.

First, **P1** or **P2** dynamers themselves did not exhibit any activity in the hydrolysis of *p*NPP (fig. S3), serving as negative controls. Moreover, **P0** showed no obvious activation effect on lipase (fig S4). Increasing the concentrations of both dynamers **P1** and **P2**, the hydrolytic efficiency of lipase was markedly enhanced (Fig. 2, A to D), achieving nearly double the lipase activity at a concentration of 0.04 mM. However, when the concentration continuously increased to 0.16 mM, a sharp decrease of lipase activity was observed, although it remained higher than the original activity, indicating an inhibition effect at a specific concentration of 0.2 mM dynamers.

The activity enhancement observed at low concentration, followed by an inhibition effect induced at a high concentration of dynamers, was not reported in previous studies in solution. It is more than evident that the interaction between lipases and dynamers is essential for enzyme activation in such complexes, which exhibit higher activates than simple lipases dissolved in aqueous solution. The formation of nanoparticles at low concentration of dynamers (<0.04 mM) provides optimal aggregates with lipase, leading, as previously observed, to water soluble complexes with a few dynamers attached to the lipase surface (Fig. 2E). This may suggest minor compression of enzyme protein structure and the interfacial configuration between the dynamers and the enzyme lid necessary for observing an activation effect.

The combined amphiphilic effects from hydrophilic PEG chain and the hydrophobic alkane chains in **3** and **4**, together with the facilitated proton relaying of the amine groups, resulted in lipase exhibiting much higher activity. This was achieved by adding an optimal amount of dynamer for creating an effective effect by simply aggregation of lipases glued by dynamers and still present on the surface of particles, being accessible to the reagents and producing a substantial activation effect (Fig. 2F). When the amount of dynamer exceeded a critical threshold, bigger aggregates, instead of stable particles, were observed in the DLS study. These aggregates may completely pack lipase and affect the accessibility of substrate to lipase, resulting in the inhibition of lipase (Fig. 2G).

## Reactivation of denatured lipases

A final set of experiments was conducted to study the impacts of dynamers on the partially and completely denatured lipases, as well as their refolding process. First, lipase was heated at high temperature for a period of time to reach a partially denatured state having only half of the original activity. Two dynamers were added both before and after the thermal treatment, and the impacts on lipase activity were examined. In all the thermal processes, no precipitation was observed in the mixed solution. When dynamers (0.02 mM) were added before the heat treatment, unfortunately, dynameric/lipase nanoparticles (fig. S5C) irreversibly collapsed/aggregated (fig. S5D), leading to similar or even higher vulnerability of the denatured lipase under confined conditions at high temperatures. In contrast, when the dynamers were added to the lipase solution after heat treatment, a notable promotion effect was further detected (Fig. 3D). The presence of **P1** increased the activity of lipase by 5-, 2.8-, and 2.3-folds after 2, 5, and 10 min at 60°C, respectively. Comparing the promotion effect of **P1** to that of the original lipase (threefold) and to partially denatured lipase (fivefold), it revealed that the presence of **P1** not only contributed to the activation of lipase but also assisted in the refolding and reactivation process of the denatured lipase (Fig. 3). Compared to **P1**, the **P2** showed lower promotion efforts on the reactivation process of denatured lipase. This phenomenon can be attributed to the more plastic behaviors of dodecyl hydrophobic component of **P2**, which may induce more rigid interactions with the exposed hydrophobic parts in lipase compared to the more fluid hexyl hydrophobic component of **P1**, making it difficult to restore the structure and activity of the thermally denatured lipase (Fig. 3, A and B).

Subsequently, the impacts of **P1** on lipase activity with different denaturation degrees were explored. Lipase was thermally treated with 60°, 65°, and 70°C for 2, 5, and 10 min, respectively. As shown in Fig. 3C, the addition of **P1** at the optimum concentration led to a lower activity promotion effect on lipase when subjected to higher temperature. For example, comparing the activity of lipase after 2 min of thermal treatment, with the presence of **P1**, the lipase pretreated under 60°C recovered to fivefold of its original activity. However, the treatment at 65°C for 2 min only led to twofold recovery of the activity, while 70°C exhibited no obvious activation effect from **P1**. Similarly, the longer time under thermal treatment, the lower promotion effect of **P1** was detected. For example, after treatment of 60°C for 2, 5, and 10 min, the activities of lipase were promoted to 5.3-, 2.8-, and 2.4-folds of its original activity, respectively. These results indicated that an increased denaturation degree of lipase corresponds to a decrease in the promotion effect of **P1** for the lipase refolding process.

Thereafter, the promotion effects of **P1** on completely denatured lipase were determined. It is well known that oxidization-reduction reagents such as glutathione [oxidized glutathione/glutathione (reduced form)] or molecular chaperones were frequently used for accelerating

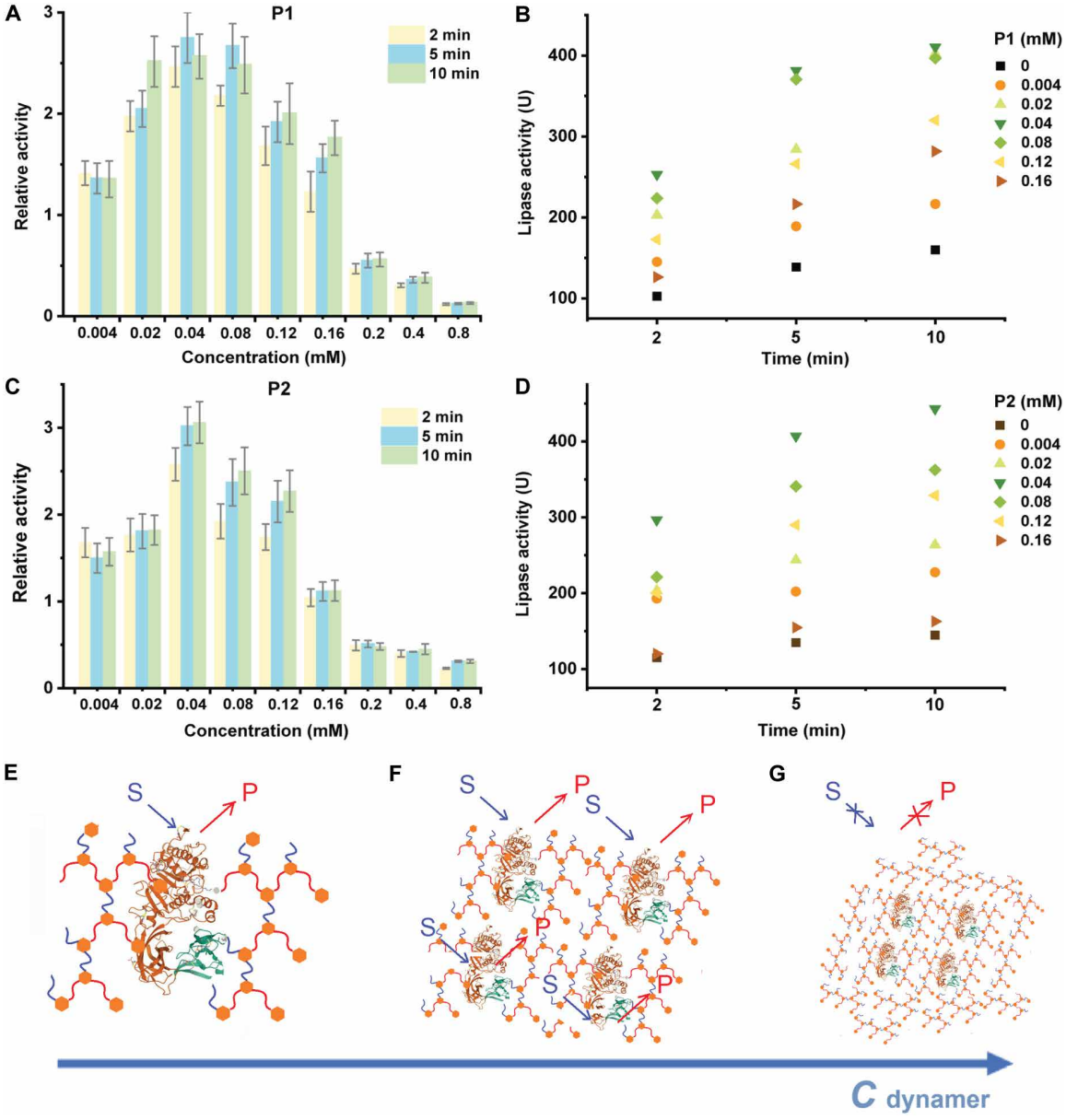


**Fig. 2. The activity enhancement effect of the dynamers on lipases and the schematic illustration of the progressive formation of dynamer-lipase complexes.** (**A** and **C**) The relative activity of lipases after incubation with dynamers of various time and concentrations, as compared to the free lipase. (**B** and **D**) The real-time hydrolysis activity of lipase with increased concentrations of **P1** and **P2**, respectively. (**E**) Illustration of low concentration of dynamers ($c < 0.04$ mM) with lipases, resulting in the formation of water-soluble species with a few dynamers attached to the surface of the lipase. (**F**) Illustration of optimal amount of dynamer ($0.04 \text{ mM} < c < 0.08$ mM) with lipases, with the aggregation of lipases glued by dynamers while the lipases are present on the surface of particles. (**G**) Illustration of exceeding critical amount of dynamer ($c > 0.16$ mM), resulting in bigger particles with lipases buried within dynameric capsules and low accessibility for the reagents. S, substrate; P, product.

the protein refolding process (*32*, *33*). In this case, 8 M guanidine hydrochloride and 40 mM dithiothreitol in a 50 mM (pH 8.0) phosphate buffer were used as the chemical denaturants, resulting in 100% lose of the original activity of lipase. After the removal of the denaturant, various concentrations of **P1** were added, and the mixtures were incubated at room temperature for 60 min to assist the refolding process of lipase. As shown in Fig. 3D, **P1** exhibited obvious promotion effects for the lipase refolding. After the incubation, the relative activity of lipase without **P1** was recovered to 2.23% of the original activity, while the addition of 0.08 mM **P1** led to 5.8-fold of the activity increase, reaching 12.97% of the relative activity. These results indicated that the refolding rate, which calculated as relative enzyme activity compared to that of lipase without chemical denaturation, was substantially improved by the addition of the dynamer **P1**.

## Lipase-dynamer interaction study

Fluorescence spectroscopy was used to detect the interactional behaviors between the dynamer and lipase. As a tryptophan-containing

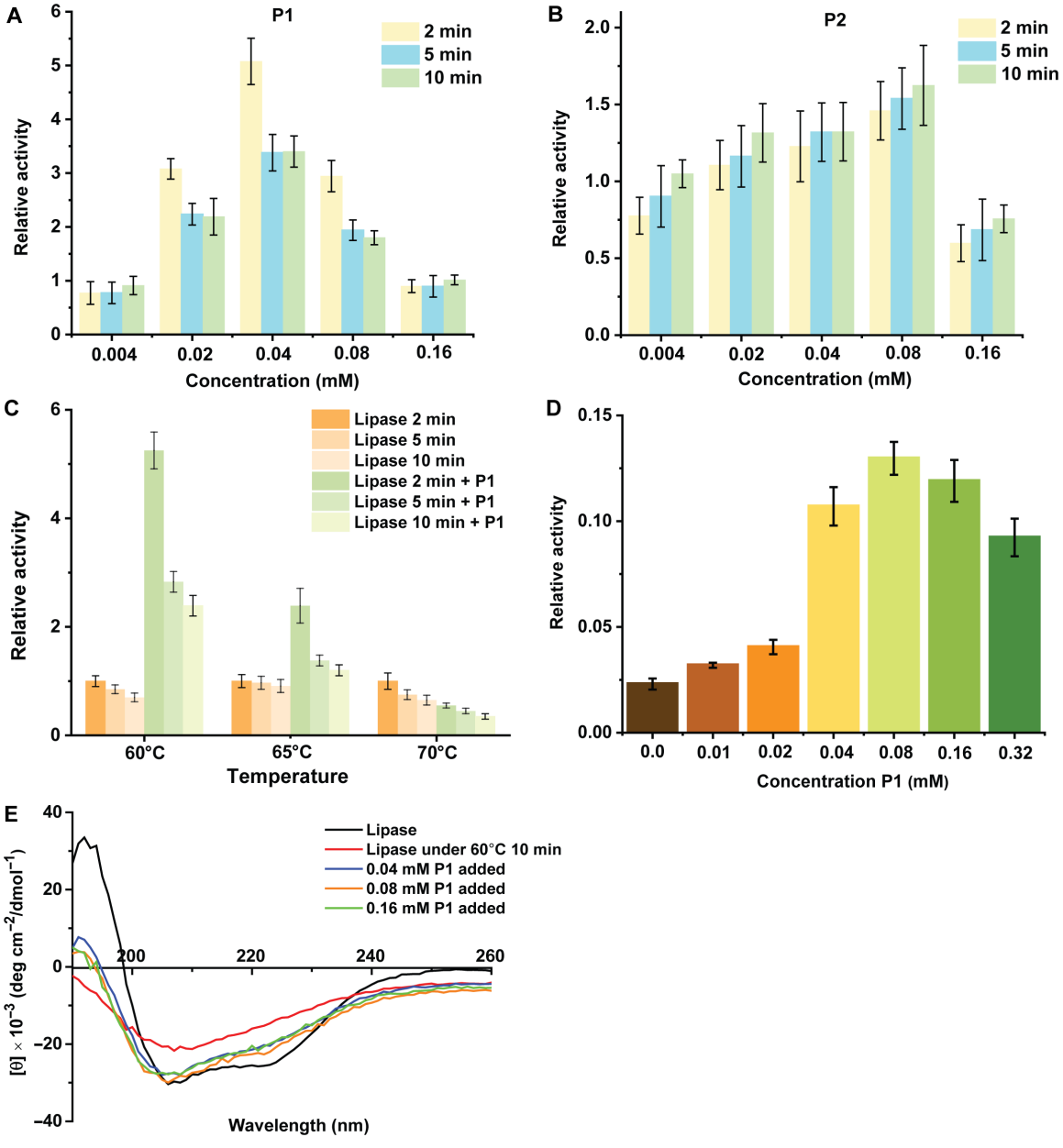


**Fig. 3. The thermostabilization and reactivation of lipases by the dynamers.** (**A** and **B**) The effect of the addition of dynamer **P1** and **P2** with increasing concentrations after heat treatment on lipase hydrolysis activity. (**C**) The promotion effect of **P1** on the lipase refolding process after thermal treatment at 60°, 65°, and 70°C. (**D**) The relative activity of lipase with the addition of different concentrations of **P1** after complete denaturation. (**E**) Circular dichroism (CD) spectra of heat-denatured lipase and heat-denatured lipase upon addition of 0.04, 0.08, and 0.16 mM **P1**.

protein, lipase has a maximum emission peak at 366 nm under the excitation wavelength of 280 nm (*34*). The UV-visible full spectra of dynamers showed maximum absorbances at 300 to 325 nm (fig. S6), thus presenting minimal interference to lipase concerning fluorescent quenching experiments. As shown in fig. S7, the fluorescence intensity of lipase decreased notably with the increasing amount of **P0**, **P1**, and **P2**. Subsequently, the association constant ($K_a$) was calculated for each dynamer, based on Stern-Volumer relation (*34*). With good fitting to the equation, **P1** (7349 $M^{-1}$) and **P2** (7169 $M^{-1}$) showed twofold higher $K_a$ values than that of **P0** (3499 $M^{-1}$) (fig. S8). Nevertheless, the reference dynamer **P0** still showed an obvious quenching effect, indicating that the interactions between lipase and dynamers may arise partly from the bonding of hydrophilic PEG to the lipase and partly from the hydrophobic interactions between hydrophobic regions in lipase and the aklyl groups in dynamers.

Circular dichroism (CD) spectroscopy was used to study the effect of dynamers on protein secondary structures. From the obtained spectra, **P1** and **P2** alone without lipase showed no obvious peaks (fig. S9). In contrast, the typical peaks of α helix and β sheet in lipase can be observed at 208 and 226 nm, respectively (fig. S10), which decreased slightly after the addition of 0.04 to 0.16 mM **P1** and **P2**, indicating the preserved typical structure of lipase. Subsequently, the

CD spectrum of denatured lipase solutions (under heat treatment at 60°C for 10 min) showed that characteristic peak of β sheet at 226 nm present decreased ellipticity, which nearly disappeared, indicating the gradual loss of typical structure of lipase. Thereafter, the addition of 0.04 to 0.16 mM **P1** to a denaturated lipase solution resulted in a gradual recovery of these characteristic peaks (Fig. 3E), demonstrating the important role of dynamer **P1** in promoting the refolding process of denatured lipase.

### Impacts of the hydrophobic alkane chains

Comparing **P1** and **P2** clearly showed that they have different impacts on the catalytic activity of lipase. Consequently, two additional dynamers, **P3** and **P4**, were synthesized with similar backbones, using 1,4-diaminobutane and 1,8-diaminooctane as hydrophobic alkane chains (fig. S12). As the result, **P3**, which has the shortest alkane chain, showed almost no effect on lipase activity across concentrations of 0.04 to 0.8 mM (fig. S13), likely due to inefficient encapsulation of lipase. Meanwhile, **P4** exhibited excellent activation of lipase at concentrations up to 0.16 mM; however, it showed unexpected decreased activity at higher concentrations, indicating substantial disruption of lipase structures due to overcrowded hydrophobic components. Moreover, both **P3** and **P4** demonstrated only minor reactivation effects on thermally denatured lipases (fig. S14), whereas **P2**, with an appropriate hydrophobic chain length, was the only dynamer that greatly enhanced the catalytic performance of lipase.

The turnover numbers here were calculated as the number of moles of substrate converted per second by one mole of enzyme active sites. As shown in table S2, the turnover number of free lipase was recorded as $2.4437 \times 10^{-7}$ μmol/s, which increased up to $8.2597 \times 10^{-7}$ μmol/s with the presence with dynamer **P1**.

Furthermore, the loading efficiency of lipase on different dynamers at various concentrations was measured. As illustrated in fig. S15, the loading efficiency of all dynamers rose from below 5% to more than 60% as the dynamer concentration increased from 0.005 to 1.0 mM. Notably, the loading efficiency increased with longer hydrophobic alkane chains in the dynamers, with the value for **P3** substantially lower than that of other dynamers, highlighting the critical role of hydrophobic chains.

### MD simulations

Modeling of *Rhizopus chinensis* lipase (RCL) was conducted at the critical micelle concentration (CMC) of its substrate *p*NPP. Thus, further MD simulations were performed to explore the impacts of dynamer **P1** on lipase catalysis, in both systems with the absence and presence of dynamer **P1**, referred as RCL-CMC$_{pNPP}$ and RCL-CMC$_{pNPP}$-**P1**, respectively. Figure 4A showed four representative snapshots during the 500-ns simulation.

Initially, the addition of dynamer into the system led to the formation of two polymeric clusters crowding the lipase, which gradually merged together and moved toward the lid region of lipase. This phenomenon is probably driven by the favorable interfacial interaction between dynamer **P1** and the hydrophobic lid, which in turn facilitated the lid opening and the access of substrate *p*NPP to the catalytic triad of lipase, resulting in a substantial activation effect.

Moreover, as illustrated in Fig. 4 and fig. S11, the presence of dynamer **P1** also induced conformational changes in RCL compared to the RCL-CMC$_{pNPP}$ system, as evidenced by alterations in root mean square deviation, root mean square fluctuation (RMSF), and solvent-accessible surface area. Specifically, the RMSF value of the lid region (Gly$^{109}$-Val$^{121}$) covering the pocket exhibited a notable decrease, suggesting conformational change. In addition, the active site of RCL transitioned from a closed conformation at 0 ns to an open state at 500 ns (Fig. 4B), thereby enhancing the accessibility of the substrate *p*NPP for subsequent catalytic reactions.

By examining the substrate-binding pocket region (Tyr$^{55}$, Gly$^{109}$-Val$^{121}$, His$^{171}$-Ala$^{176}$, and His$^{284}$) of RCL, which was covered by the lid, its hydrophilic surface area (SA$_{philic}$) and hydrophobic surface area (SA$_{phobic}$) were compared on the basis of the amino acid properties. As shown in Fig. 4C, the presence of dynamer **P1** resulted in a higher SA$_{phobic}$ value in the substrate-binding pocket of lipase, indicating increased exposure of the pocket, probably owing to the lid movement upon the binding to dynamer **P1**. These simulation results correlated well with the phenomenon of interfacial activation (*35*, *36*) and supported our earlier speculation inferred from Fig. 2.

Furthermore, two distinguished conformations of RCL, with open and closed lid, were analyzed during the MD simulation. Consequently, compared to the RCL-CMC$_{pNPP}$ system, the presence of dynamer **P1** substantially extended the exposure time of the catalytic triad residues, particularly Ser$^{172}$, during the 500-ns simulation (fig. S11D). It is well known that lipase can be fixed into an open structure upon contact with a hydrophobic surface, facilitating exposure of the active center. Therefore, lipases in their open forms have been selectively immobilized on various hydrophobic supports to improve their activity and stability (*37*–*39*). In this study, the synthetic dynamer served as an effective hydrophobic support, leading to aggregated lipases on the surface of the dynamer particles, while the open structure of lipase can be easily maintained.

## DISCUSSION

In the current work, we present a simple and effective method to promote lipase activity and restore the thermally and chemically denatured lipase by direct addition of functional amphiphilic dynamers into the enzyme reaction solution. Owing to the interfacial activation of lipase, the coexistence of hydrophilic and hydrophobic components within dynamers led to an obvious enhancement of lipase activity. By adjusting the ratio of PEG chain and diamine monomers, as well as the length of alkane chain in diamine monomer, we can regulate the hydrophilicity and hydrophobicity of dynamers, as well as their interaction strength and activation effects for lipase. Moreover, the dynamers can encapsulate the enzyme into the nanoparticulate catalytic complex through the multivalent dynameric cross-linking, facilitating close biochemical reaction in a physiological cell media. The dynameric cross-linking and protective confinement for lipase enhance its catalytic activity and also promote the refolding process of the folded, partially denatured, and completely but reversibly denatured lipase. Molecular simulation studies demonstrated conformational change of lipase upon the presence of dynamer **P1**, leading to prolonged exposure of lipase active center and improved substrate accessibility. This strategy has successfully provided an important prospect and approach for the improvement of lipase performance.

## MATERIALS AND METHODS

### Materials

Benzene-1,3,5-tricarbaldehyde was purchased from Energy Chemical. PEG-bis-(3-aminopropyl)-terminated, 1,6-hexanediamine, and 1,12-dodecane diamine were obtained from Sigma-Aldrich and used

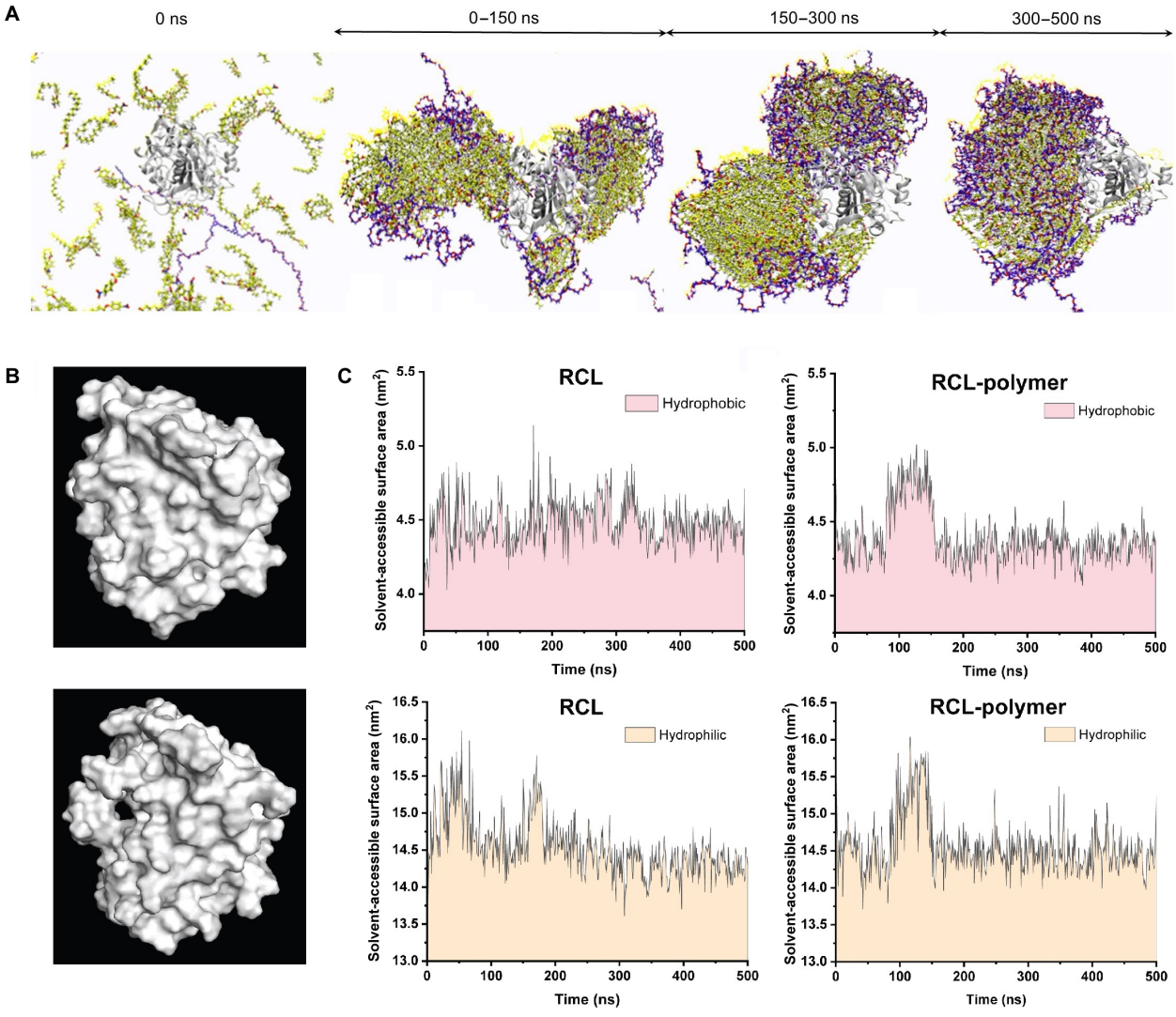


**Fig. 4. The study of lipase activation mechanisms by using MD simulations.** (**A**) The snapshots of RCL backbones in RCL-CMC$_{pNPP}$-dynamer system at 0, 150, 300, and 500 ns. The gray cartoon model represents RCL, and the yellow and blue molecules represent the substrate *p*NPP and the dynamer, respectively. (**B**) The simulated RCL conformations at 0 and 500 ns. (**C**) SA$_{philic}$ of the pocket region of lipase in RCL-CMC$_{pNPP}$ system and RCL-CMC$_{pNPP}$-**P1** system during the 500-ns simulations; SA$_{phobic}$ of the pocket region of lipase in RCL-CMC$_{pNPP}$ system and RCL-CMC$_{pNPP}$-**P1** system during the 500-ns simulations.

as received. Other chemicals and solvents were purchased commercially and used without further purification.

### Synthesis of the dynamers

The dynamers were prepared by dissolving benzene-1,3,5-tricarbaldehyde (**1**, 0.1 mmol) in 10-ml dried methanol, followed by addition of PEG-bis-(3-aminopropyl)-terminated (**2**, 0.075 mmol) and 1,6-hexanediamine (**3**, 0.075 mmol, for **P1**) or 1,12-dodecanediamine (**4**, 0.075 mmol, for **P2**) or 1,4-diaminobutane (0.075 mmol, for **P3**) or 1,8-diaminooctane (0.075 mmol, for **P4**). After stirring at 60°C for 18 hours to reach equilibrium, the solvent was then removed and replaced by 10 ml of distilled $H_2O$ to prepare the stock solutions.

### Gel permeation chromatography

GPC coupled with the refractive index detector and an 18-angle multi-angle laser scattering detector (MALS) (Wyatt) was used to determine the molecular weight of the dynamers. $NaBH_4$ (4.8 mg) was added to 2 ml of each dynamer solution in water and stirred for 10 min, followed by addition of 2 ml of $H_2O$ and removal of the solvent by evaporation to 25% volume. After acidiation with 5% HCl to adjust pH to 2.0, followed by the addition of 20% NaOH to adjust pH from 12.0 to 13.0, the products were extracted with $CHCl_3$, which were weighed and dissolved in the mobile phase (0.2 M NaCl) to prepare samples (5 mg/ml) for GPC.

### DLS and TEM size analysis

Size analysis of complexes with different lipase/dynamer ratios was carried out by a DLS method. The procedure was started by adding 5 μl of purified lipase to 1995 μl of PBS buffer [50 mM (pH 8.0)] in a 2-ml quartz cuvette, with the initial size of pure lipase measured. Then, an increasing amount of dynamers (0.0005, 0.0025, 0.005, 0.01, 0.025, 0.05, 0.1, 0.25, and 0.5 μl) was added into the cuvette respectively

to measure the size of complexes. The average hydrodynamic diameter and polydispersity index of complexes at 25°C were determined using a DLS detector (4-mW laser, 633-nm incident beam, 90° scattering angle). Values were given as mean ± SD of three measurements.

TEM was used to confirm the morphology and particle sizes. Ten microliters of 0.01 mM **P1** and **P2** solution as well as the dynamer/lipase complex (containing 0.01 mM dynamer) were retrieved to a coated copper wire. After evaporation in air, the TEM images were recorded by an 80-kV TEM.

### Determination of the activation effects

The influence of dynamers on lipase catalytic reactivity was evaluated using a UV spectrophotometer to detect the absorbance of *p*-NP at 410 nm, which was produced by hydrolysis reaction of *p*NPP. The stock solution of *p*NPP was prepared by dissolving 0.015 g of *p*NPP into mixed solution of 5 ml of isopropanol and 45 ml of 50 mM phosphate buffer (pH 8.0). Then, a 100-μl lipase (100 U) in PBS solution (50 mM) was added to 2.4-ml substrate solution to initiate the hydrolytic reaction. The influences of dynamers on lipase activity were assessed by adding an increasing amount of dynamer solution. After 2-, 5-, and 10-min reaction, the absorbance of hydrolyzed *p*-NP at 410 nm was recorded. Then, the results were calculated as relative enzyme activity compared with the result of the reaction of lipase alone, which was set as 100%. Control experiments without the presence of lipase were also carried out to check the hydrolysis of dynamers alone.

### Activity restoration of the denatured lipases

More experiments were carried out to explore the activation effect of **P0**-**P2** on partially denaturated lipase (by heat treatment) and completely denaturated lipase (by chemical denaturant). The activity restoration effects of the dynamers on denaturated lipase were also determined using the *p*NPP method mentioned above. After lipase denaturation by thermal or chemical methods, increasing concentation of dynamers (0.004, 0.02, 0.04, 0.08, 0.12, and 0.16 mM) was added to reaction solution. Then, the results were calculated as relative enzyme activity compared with the result of the reaction of lipase alone, which taken as 100%.

### Loading efficiency of lipase to dynamers

Liapse solution was prepared initially with the concentration of 0.05331 mg/ml, followed by addition of dynamers to achieve the final dynamer concentrations of 0.005, 0.02, 0.05, 0.1, 0.2, 0.4, 0.66, and 1.0 mM. The solutions were left incubated for 20 min. Thereafter, the solutions were centrifuged at 12,000 rpm for 10 min, with the supernatant collected to determine the protein concentration by the Bradford method (*40*).

### Lipase-dynamer binding studies by fluorescence measurements

Purified lipase (from *Rhizupos Chinensis* CCTCC M201021) was dissolved in PBS buffer solution [50 mM (pH 8.0)] with a protein concentration of about 50 μM. The procedure was started by adding 5 μl of lipase solution to 1500 μl of PBS buffer [50 mM (pH 8.0)] in a 2-ml quartz cuvette. The fluorescence emmision intensities were measured from 280 to 500 nm with the excitation wavelength of 280 nm. The Stern-Volmer relation ($I_0/I = 1 + K_a [P]$) was used to calculate the $K_a$. The values in the highest fluorescence intensity of lipase at 366 nm were used and applied to the relation. $I_0$ and $I$ stand for the initial fluorescence intensity of lipase alone and the intensity of lipase with the presence of dynamers. [$P$] is the dynamer concentrations.

### CD studies

The CD spectra were recorded at wavelengths from 190 to 250 nm, using an Xe lamp (100 W) and a 1-mm path length quartz cuvette, at a speed of 60 nm/min. All observed CD spectra were baseline-subtracted for PBS buffer [50 mM (pH 8.0)]. The CD spectrum of lipase alone was recorded by transferring a 400-μl sample composed of 25 μl of lipase stocking solution (50 μM) diluted by 375-μl PBS buffer [50 mM (pH 8.0)]. Then, the increasing amounts of **P1**/**P2** (0.02, 0.04, 0.08, and 0.16 mM) were added respectively. The final data were averaged from three measurements.

### Molecular modeling and MD simulation studies

The x-ray crystal structure of RCL (Protein Data Bank ID: 6A0W, 2.0 Å) obtained from the RCSB Protein Data Bank was used in this study. AmberTools18 was used to generate polymer parameter files and topological files for the simulations. The molecular structures of the polymers were optimized with Gaussian 16. GROMACS Package (version 2019.6) was used to perform all MD simulations. The force field AMBER14SB + parmbsc133 and general Amber force field 34 were used for all of the simulations. In addition, disulfide bond restraints were generated for the lipase disulfide bonds ($Cys^{56}$-$Cys^{295}$, $Cys^{67}$-$Cys^{70}$, and $Cys^{262}$-$Cys^{271}$).

The MD was performed under two systems. The first was referred as the lipase-$CMC_{pNPP}$ system, in which the lipase was placed in a 16 nm–by–16 nm–by–16 nm cubic simulation box filled with water and 200 *p*NPP molecules to represent the micelle concentration of *p*NPP. The other simulation system was referred as the lipase-polymer-$CMC_{pNPP}$ system, in which lipase was placed in a cubic simulation box filled with water and 200 *p*NPP molecules, as well as 8 polymer molecules to represent the lipase-polymer-$CMC_{pNPP}$ system with the optimum concentration (0.04 mM) of polymer to promote lipase activity.

Periodic boundary conditions were set in the $x$, $y$, and $z$ directions. Neutralization of the system was carried out by replacing water molecules with $Na^+$ and $Cl^-$ ions. The steepest descent energy minimization was used in the first 500 steps, and the conjugate gradient method was used in the last 2000 steps. After energy minimization, 2 ns of constant number of particles, volume, and temperature (NVT) equilibration at 313 K was performed. Bond length constraints were applied to H-bonds based on Linear Constraint Solver (LINCS) for molecular simulations with bond constraints. Long-range electrostatic effects were handled using particle mesh Ewald (PME) and temperature coupling was performed using velocity rescaling with a stochastic term.

During heating, position restraints with a force constant of 10.0 kcal/mol per $Å^2$ were imposed on lipase. After NVT equilibration, 5 ns of constant number of particles, pressure, and temperature (NPT) equilibration at 313K was performed. The Berendsen's method was used for pressure coupling. The cutoff distance for van der Waals interactions was 10.0 Å. After NPT equilibration, 200-ns production simulations were performed on both systems. Pressure coupling was applied using the Parrinello-Rahman method.

## Supplementary Materials

**The PDF file includes:**

Supplementary Text
Figs. S1 to S15

Tables S1 and S2
Legend for movie S1

**Other Supplementary Material for this manuscript includes the following:**
Movie S1

## REFERENCES AND NOTES


1. S. Wu, Y. Zhou, T. Wang, H.-P. Too, D. I. C. Wang, Z. Li, Highly regio- and enantioselective multiple oxy- and amino-functionalizations of alkenes by modular cascade biocatalysis. *Nat. Commun.* **7**, 11917 (2016).
2. E. L. Bell, W. Finnigan, S. P. France, A. P. Green, M. A. Hayes, L. J. Hepworth, S. L. Lovelock, H. Niikura, S. Osuna, E. Romero, K. S. Ryan, N. J. Turner, S. L. Flitsch, Biocatalysis. *Nat. Rev. Methods Primers* **1**, 46 (2021).
3. P. Intasian, K. Prakinee, A. Phintha, D. Trisrivirat, N. Weeranoppanant, T. Wongnate, P. Chaiyen, Enzymes, in vivo biocatalysis, and metabolic engineering for enabling a circular economy and sustainability. *Chem. Rev.* **121**, 10367–10451 (2021).
4. S. Wu, R. Snajdrova, J. C. Moore, K. Baldenius, U. T. Bornscheuer, Biocatalysis: Enzymatic synthesis for industrial applications. *Angew. Chem., Int. Ed. Engl.* **60**, 88–119 (2021).
5. S. Soni, Trends in lipase engineering for enhanced biocatalysis. *Biotechnol. Appl. Biochem.* **69**, 265–272 (2022).
6. P. T. Bandeira, J. C. Thomas, A. R. M. de Oliveira, L. Piovan, Lipase-mediated kinetic resolution: An introductory approach to practical biocatalysis. *J. Chem. Educ.* **94**, 800–805 (2017).
7. G. Angajala, P. Pavan, R. Subashini, Lipases: An overview of its current challenges and prospectives in the revolution of biocatalysis. *Biocatal. Agric. Biotechnol.* **7**, 257–270 (2016).
8. K. Świderek, S. Velasco-Lozano, M. À. Galmés, I. Olazabal, H. Sardon, F. López-Gallego, V. Moliner, Mechanistic studies of a lipase unveil effect of pH on hydrolysis products of small PET modules. *Nat. Commun.* **14**, 3556 (2023).
9. Y. Zhang, P. Vongvilai, M. Sakulsombat, A. Fischer, O. Ramström, Asymmetric synthesis of substituted thiolanes through domino Thia-Michael–Henry dynamic covalent systemic resolution using lipase catalysis. *Adv. Synth. Catal.* **356**, 987–992 (2014).
10. J. Xu, Y. Cen, W. Singh, J. Fan, L. Wu, X. Lin, J. Zhou, M. Huang, M. T. Reetz, Q. Wu, Stereodivergent protein engineering of a lipase to access all possible stereoisomers of chiral esters with two stereocenters. *J. Am. Chem. Soc.* **141**, 7934–7945 (2019).
11. K. Liebeton, A. Zonta, K. Schimossek, M. Nardini, D. Lang, B. W. Dijkstra, M. T. Reetz, K.-E. Jaeger, Directed evolution of an enantioselective lipase. *Chem. Biol.* **7**, 709–718 (2000).
12. G. Druteika, M. Sadauskas, V. Malunavicius, E. Lastauskiene, L. Taujenis, A. Gegeckas, R. Gudiukaite, Development of a new *Geobacillus* lipase variant GDlip43 via directed evolution leading to identification of new activity-regulating amino acids. *Int. J. Biol. Macromol.* **151**, 1194–1204 (2020).
13. R. Wang, S. Wang, Y. Xu, X. Yu, Enhancing the thermostability of *Rhizopus chinensis* lipase by rational design and MD simulations. *Int. J. Biol. Macromol.* **160**, 1189–1200 (2020).
14. P. Qu, R. Lazim, D. Li, R. Xu, F. Wang, X. Li, Y. Zhang, Enhancing methanol tolerance of *Thermomyces lanuginosus* lipase by rational design and biodiesel production through one-step feeding of methanol. *J. Clean. Prod.* **450**, 141949 (2024).
15. X. Cai, J.-W. Shen, Y. Qiang, J. Hua, Z.-Q. Ma, Z.-Q. Liu, Y.-G. Zheng, Efficient activity enhancement of a lipase from sporisorium reilianum for the synthesis of a moxifloxacin chiral intermediate via rational design. *Engineering* **19**, 207–216 (2022).
16. W. Chong, Y. Qi, L. Ji, Z. Zhang, Z. Lu, B. Nian, Y. Hu, Computer-aided tunnel engineering: A promising strategy for improving lipase applications in esterification reactions. *ACS Catal.* **14**, 67–83 (2024).
17. L. He, C. Zeng, L. Wei, L. Xu, F. Song, J. Huang, N. Zhong, Fabrication of immobilized lipases for efficient preparation of 1,3-dioleoyl-2-palmitoylglycerol. *Food Chem.* **408**, 135236 (2023).
18. S. Y. Zaitsev, A. A. Savina, I. S. Zaitsev, Biochemical aspects of lipase immobilization at polysaccharides for biotechnology. *Adv. Colloid Interface Sci.* **272**, 102016 (2019).
19. K. Zhao, X. Cao, Q. Di, M. Wang, H. Cao, L. Deng, J. Liu, F. Wang, T. Tan, Synthesis, characterization and optimization of a two-step immobilized lipase. *Renew. Energy* **103**, 383–387 (2017).
20. S. Mortazavi, H. Aghaei, Make proper surfaces for immobilization of enzymes: Immobilization of lipase and α-amylase on modified Na-sepiolite. *Int. J. Biol. Macromol.* **164**, 1–12 (2020).
21. J. Noro, A. Cavaco-Paulo, C. Silva, Chemical modification of lipases: A powerful tool for activity improvement. *Biotechnol. J.* **17**, e2100523 (2022).
22. N. S. Rios, E. G. Morais, W. dos Santos Galvão, D. M. Andrade Neto, J. C. S. dos Santos, F. Bohn, M. A. Correa, P. B. A. Fechine, R. Fernandez-Lafuente, L. R. B. Gonçalves, Further stabilization of lipase from *Pseudomonas fluorescens* immobilized on octyl coated nanoparticles via chemical modification with bifunctional agents. *Int. J. Biol. Macromol.* **141**, 313–324 (2019).
23. P. Abellanas-Perez, D. Carballares, R. Fernandez-Lafuente, J. Rocha-Martin, Glutaraldehyde modification of lipases immobilized on octyl agarose beads: Roles of the support enzyme loading and chemical amination of the enzyme on the final enzyme features. *Int. J. Biol. Macromol.* **248**, 125853 (2023).
24. Y. Zhang, Y.-M. Legrand, E. Petit, C. T. Supuran, M. Barboiu, Dynamic encapsulation and activation of carbonic anhydrase in multivalent dynameric host matrices. *Chem. Commun.* **52**, 4053–4055 (2016).
25. Y. Zhang, W.-X. Feng, Y.-M. Legrand, C. T. Supuran, C.-Y. Su, M. Barboiu, Dynameric host frameworks for the activation of lipase through H-bond and interfacial encapsulation. *Chem. Commun.* **52**, 13768–13770 (2016).
26. Y. Zhang, M. Barboiu, O. Ramström, J. Chen, Surface-directed selection of dynamic constitutional frameworks as an optimized microenvironment for controlled enzyme activation. *ACS Catal.* **10**, 1423–1427 (2020).
27. D.-D. Su, K. Aissou, Y. Zhang, V. Gervais, S. Ulrich, M. Barboiu, Squalene–polyethyleneimine–dynamic constitutional frameworks enhancing the enzymatic activity of carbonic anhydrase. *Catal. Sci. Technol.* **12**, 3094–3101 (2022).
28. D. Su, Y. Zhang, S. Ulrich, M. Barboiu, Constitutional dynamic inhibition/activation of carbonic anhydrases. *ChemPlusChem* **86**, 1500–1510 (2021).
29. S. Wang, Y. Xu, X.-W. Yu, Propeptide in *Rhizopus chinensis* lipase: New insights into its mechanism of activity and substrate selectivity by computational design. *J. Agric. Food Chem.* **69**, 4263–4275 (2021).
30. T. de Andrade Silva, W. J. Keijok, M. C. C. Guimarães, S. T. A. Cassini, J. P. de Oliveira, Impact of immobilization strategies on the activity and recyclability of lipases in nanomagnetic supports. *Sci. Rep.* **12**, 6815 (2022).
31. J. Wang, M. Zhao, T. Liu, F. Feng, A. Zhou, Guidelines for the digestive enzymes inhibition assay. *eFood* **3**, e31 (2022).
32. L. Ito, M. Okumura, K. Tao, Y. Kasai, S. Tomita, A. Oosuka, H. Yamada, T. Shibano, K. Shiraki, T. Kumasaka, H. Yamaguchi, Glutathione ethylester, a novel protein refolding reagent, enhances both the efficiency of refolding and correct disulfide formation. *Protein J.* **31**, 499–503 (2012).
33. A. P. Ben-Zvi, P. Goloubinoff, Review: Mechanisms of disaggregation and refolding of stable protein aggregates by molecular chaperones. *J. Struct. Biol.* **135**, 84–93 (2001).
34. J. Keizer, Nonlinear fluorescence quenching and the origin of positive curvature in Stern-Volmer plots. *J. Am. Chem. Soc.* **105**, 1494–1498 (1983).
35. J. Zhang, Z. Wang, W. Zhuang, H. Rabiee, C. Zhu, J. Deng, L. Ge, H. Ying, Amphiphilic nanointerface: Inducing the interfacial activation for lipase. *ACS Appl. Mater. Interfaces* **14**, 39622–39636 (2022).
36. S. Wang, Y. Xu, X.-W. Yu, A phenylalanine dynamic switch controls the interfacial activation of *Rhizopus chinensis* lipase. *Int. J. Biol. Macromol.* **173**, 1–12 (2021).
37. Y. Sugimura, K. Fukunaga, T. Matsuno, K. Nakao, M. Goto, F. Nakashio, A study on the surface hydrophobicity of lipases. *Biochem. Eng. J.* **5**, 123–128 (2000).
38. J. He, Y. Xu, H. Ma, Q. Zhang, D. G. Evans, X. Duan, Effect of surface hydrophobicity/hydrophilicity of mesoporous supports on the activity of immobilized lipase. *J. Colloid Interface Sci.* **298**, 780–786 (2006).
39. H. T. Deng, J. J. Wang, M. Ma, Z. Y. Liu, F. Zheng, Hydrophobic surface modification of chitosan gels by stearyl for improving the activity of immobilized lipase. *Chin. Chem. Lett.* **20**, 995–999 (2009).
40. M. M. Bradford, A rapid and sensitive method for the quantitation of microgram quantities of protein utilizing the principle of protein-dye binding. *Anal. Biochem.* **72**, 248–254 (1976).


**Acknowledgments**
**Funding:** This work was supported by the following funding: National Natural Science Foundation of China (NSFC) 22008090 (Y.Z.) and 31671799 (X.Y.), National Key R&D Program of China 2021YFC2103100 (J.C.), Six Talent Peaks Project in Jiangsu Province NY-010 (X.Y.), 111 Project 111-2-06 (X.Y.), and Natural Science Foundation of Jiangsu Province BK20180625 (Y.Z.)
**Author contributions:** Conceptualization: Y.Z. and M.B. Methodology: R.W., S.W., and J.C. Investigation: R.W. and S.W. Visualization: R.W. and S.W. Supervision: Y.Z., X.Y., and Y.X. Funding acquisition: Y.Z., J.C., and X.Y. Writing—original draft: R.W. and S.W. Writing—review and editing: Y.Z., M.B., and X.Y. **Competing interests:** The authors declare that they have no competing interests. **Data and materials availability:** All data needed to evaluate the conclusions in the paper are present in the paper and/or the Supplementary Materials.

Submitted 4 September 2024
Accepted 5 February 2025
Published 12 March 2025
10.1126/sciadv.ads9371